# $K_A$-Band Weather-Dependent System Performance Estimates for Goldstone

R. C. Clauss
TDA Technology Development

M. M. Franco and S. D. Slobin
Radio Frequency and Microwave Subsystems Section

*A $K_A$-band atmospheric noise temperature and attenuation statistical model is developed for Goldstone, based on water vapor radiometer measurements at 31.4 GHz made during winter and spring 1981. An equivalent X-band model is derived from these measurements, and the two sets of data are compared to determine the possible advantages of developing DSN telecommunications links at 32 GHz. For a nominal elevation angle of 30 degrees and identical antennas, it is found that a $K_A$-band system at Goldstone will show a 5 to 10 dB signal-to-noise ratio advantage over an X-band system more than 99 percent of the time.*

## I. Introduction

Previous studies (Refs. 1 and 2) have shown the advantages and feasibility of developing a DSN communications link at $K_A$-band (32 GHz). Existing communications frequencies are at S-band (2.3 GHz) and X-band (8.5 GHz), and operation in these bands has proven to be spectacularly successful as can be seen, for example, by the number and quality of pictures taken by the two Voyager spacecraft at Jupiter and Saturn. A description of the Voyager Telecommunications System is given in Ref. 3. As future spacecraft send back data from farther and farther into space, methods will have to be developed to receive their progressively weaker signals.

The signal-to-noise ratio on the ground in a telecommunications link (for a 1-Hz bandwidth) may be defined by the equation (Ref. 3):

$$SNR = \frac{P_T A_T A_R f^2}{c^2 R^2 L_a k T_s L_s} \qquad (1)$$

where

$P_T$ = spacecraft transmitted power, W

$A_T$ = spacecraft antenna effective area, $m^2$

$A_R$ = ground receiving antenna effective area, $m^2$

$f$ = frequency, Hz

$c$ = velocity of light, $3 \times 10^8$ m/sec

$R$ = distance from antenna to spacecraft, m

$L_a$ = atmospheric loss factor, ratio > 1.0

$k$ = Boltzmann's constant, $1.38 \times 10^{-23}$ joules/K

$T_s$ = system equivalent noise temperature, K

$L_s$ = all other attenuation mechanisms other than the atmosphere, ratio > 1.0

As the maximization of SNR is a goal of any telecommunications system, all factors in Eq. (1) are constantly being examined in an attempt to increase those in the numerator and decrease those in the denominator. Clearly it is desirable to increase spacecraft transmitter power and antenna area (to increase gain) and to increase ground antenna size so as to intercept more of this larger and more concentrated signal. Not so obvious is the interaction among the factors $f^2$, $L$, and $T_s$, all of which are related to frequency. As frequency increases, so do the losses due to the atmosphere (in general) and so does the system noise temperature. The one-to-one correspondence between attenuation and noise temperature is given by the relationship (Ref. 4).

$$T_a = T_p (1 - 1/L) \tag{2}$$

where

$T_a$ = atmospheric noise temperature (one component of system noise temperature), K

$T_p$ = equivalent physical temperature of the attenuating atmosphere, K

$L$ = atmospheric loss factor, $10^{A\,(\mathrm{dB})/10}$, ratio > 1.0

$A$(dB) = attenuation of the atmosphere, dB

Further discussions of atmospheric noise temperature concepts and the statistics of actual Goldstone X-band measurements are given in Refs. 5-7.

An attempt to develop a 32-GHz noise temperature model by extrapolating 8.5-GHz statistics will lead to large errors due to accuracy uncertainties at the lower frequency. Cloud and rain effects scale by frequency squared over the microwave frequency range, and, coincidentally, water vapor effects at 8.5 and 32 GHz also have a nearly $f^2$ relationship. As $f^2 = 14.2$ for these two frequencies, uncertainties of 1 K at X-band model to 14 K uncertainties at $K_A$-band. Thus for comparison of X and $K_A$-band systems, $K_A$-band measurements (which can be made with accuracies comparable to X-band) can be used to derive an accurate X-band model.

## II. Calculation of the Models

A two-channel water vapor radiometer (WVR) was used at Goldstone (DSS 13) to measure the increase in sky brightness (noise) temperature caused by tropospheric effects at 31.4 GHz. The second WVR channel operated at 20.6 GHz. These measurements were carried out during February through April 1982 and appear to be typical of the "rainy" period of the year in the desert. The average total yearly rain in the Mojave Desert is about 3.5 inches, compared with 20 inches in Madrid and 26 inches in Canberra, the locations of the other two DSN 64-m antennas.

For the purposes of this report, it will be assumed that the 31.4-GHz measurements accurately reflect measurements which would have been made at 32 GHz. In addition to the 1500 hours of measured noise temperature data, humidity data from one year's radiosonde runs at Edwards Air Force Base (also a California desert location) were used to generate yearly statistics of water vapor noise temperature effects. The measured $K_A$-band data were judiciously expanded (tripled) to create a fictitious six-month-long "winter," to ensure a worst-case analysis. It was assumed that the highest noise temperatures due to water vapor (radiosonde measurements) occurred in the summer and fall and were independent of the rain events. Both the water vapor data and $K_A$-band data were thus merged to create a year model of noise temperature statistics for a Goldstone atmosphere and a 30-degree radiometer elevation angle. The cumulative distribution for this model is given in line 1 of Table 1. (Cumulative distribution is the percent time a measurement is less than or equal to a particular value.)

Table 1 shows the complete series of calculations carried out to develop $K_A$- and X-band noise temperature, attenuation, and SNR models. Line 2 gives the $K_A$-band model developed from Goldstone noise temperature measurements and radiosonde data. The value 9.84 K is the oxygen-only baseline as given in Ref. 7; the Goldstone measurements were made relative to the clear, dry baseline. Line 3 gives the "wet" contribution of water vapor, clouds, and rain (line 2 minus oxygen). Clouds and rain have a frequency-squared relationship, and for the frequencies considered, so does water vapor. The X-band "wet" contribution (line 4) can be obtained by dividing line 3 by 14.2 ($f^2 = (32/8.5)^2 = 14.2$). The total X-band contribution (line 5) is obtained by adding X-band oxygen (3.54 K, Ref. 7) to line 4. Using Eq. (2) and a mean atmospheric physical temperature of 10°C (283.16 K), it is found that 0.1 dB loss results in a 6.45 K noise temperature contribution. Applying this rule-of-thumb factor to lines 2 and 5 yields $K_A$- and X-band atmospheric attenuations at 30-deg elevation (lines 6 and 7).

Table 2 presents the noise temperature values which will be appropriate for 1985-era Deep Space Network receiving systems. Values in this table are added to lines 2 and 5 to obtain total $K_A$- and X-band system noise temperatures (lines 8 and 9). These system noise temperature cumulative distributions are shown in Fig. 1. The attenuation above the clear, dry baseline (lines 10 and 11) is obtained by dividing the "wet" contributions (lines 3 and 4) by 6.45 K/0.1 dB.

For a given system, the SNR degradation from baseline conditions caused by increased atmospheric noise temperature and attenuation is given by

$$\Delta SNR = 10 \log_{10} [T_{system}/T_{base}] + \Delta dB \quad (3)$$

where

$T_{system}$ = system noise temperature, K (lines 8, 9)

$T_{base}$ = baseline system noise temperature, K (lines 8, 9 at 0%).

$\Delta dB$ = attenuation above clear, dry baseline, dB (lines 10, 11)

The ΔSNR results are shown in lines 12 and 13. For receiving systems described in Table 2, and with antennas of the same gain, it can be seen that a $K_A$-band system shows much inferior SNR performance than does an X-band system. Line 14 shows a direct SNR degradation comparison of $K_A$- and X-band systems as given by

$$\Delta SNR\,(K/X) = -10 \log_{10} \frac{T_{system}, K}{T_{system}, X} - (A_K - A_X) \quad (4)$$

where

$T_{system}$ = lines 8, 9

$A_K$ = line 6

$A_X$ = line 7

Even under clear, dry conditions (0%), the $K_A$-band system appears to be inferior to an X-band system due to higher attenuation and noise temperature (all other things being equal). Then from where does the advantage of $K_A$-band over X-band come? It is the $f^2$ factor in Eq. (1). For transmitting antennas of equal size and receiving antennas of equal size with "perfect" surfaces, the net advantage of operating at higher frequencies increases as $f^2$ (or 11.51 dB for 32 and 8.5 GHz). When this 11.51 dB is factored into the equation for SNR, it can be seen (line 15) that for adverse weather conditions that are exceeded only 0.5% of the time (cumulative distribution = 99.5%) the $K_A$-band system still retains a 5-dB advantage over X-band. For more benign weather conditions this advantage increases. Figure 2 shows the distribution of $K_A$-band SNR advantage relative to X-band for Goldstone and a 30-deg elevation angle. This curve is read, for example, "90-percent of the time the $K_A$-band SNR advantage over X-band exceeds 8.20 dB, up to a maximum of 10.62 dB."

## III. Conclusion

It is seen from the models developed that a $K_A$-band system retains a substantial SNR advantage (at least 5 dB) over an X-band system more than 99 percent of the time at Goldstone. This, of course, depends on equal antenna and transmitter performance at the two frequencies. Even if the hybrid $K_A$-band model is somewhat in error, the X-band model is derived from it and both will be "wrong" in the same way. From the analysis presented here, it can be seen that for Goldstone, at least, operations at $K_A$-band will not be limited by the troposphere. For the overseas DSN locations, where the weather is far more severe, the advantage will not be so large for such a large percentage of the time. Atmospheric noise temperature measurements at both $K_A$- and X-band must be made at the overseas sites to develop models and system performance estimates there also.

# References

1. Potter, P. D., "64-Meter Antenna Operation at $K_A$-Band," *TDA Progress Report 42-57*, pp. 65-70, Jet Propulsion Laboratory, Pasadena, Calif., June 15, 1980.

2. Potter, P. D., "Use of $K_A$-Band for Radio Metric Determinations," *TDA Progress Report 42-58*, pp. 59-66, Jet Propulsion Laboratory, Pasadena, Calif., Aug. 15, 1980.

3. Edelson, R. E., et al., "Voyager Telecommunications: The Broadcast from Jupiter", *Science*, Vol. 204, pp. 913-921, June 1, 1979.

4. Slobin, S. D., "Microwave Noise Temperature and Attenuation of Clouds at Frequencies Below 50 GHz," JPL Publication 81-46, Jet Propulsion Laboratory, Pasadena, Calif., July 1, 1981.

5. Slobin, S. D., et al., "X-Band Atmospheric Noise Temperature Statistics at Goldstone, DSS 13, 1975-1976," *DSN Progress Report 42-38*, pp. 70-76, Jet Propulsion Laboratory, Pasadena, Calif., Apr. 15, 1977.

6. Slobin, S. D., et al., "X-Band Atmospheric Noise Temperature Data and Statistics at Goldstone, DSS 13, 1977-1978," *DSN Progress Report 42-52*, pp. 108-116, Jet Propulsion Laboratory, Pasadena, Calif., Aug. 15, 1979.

7. Slobin, S. D., et al., "X-Band Atmospheric Noise Temperature Statistics at Goldstone, DSS 13, 1979 and 1980, and Clear Air Noise Temperature Models for Goldstone," *TDA Progress Report 42-64*, pp. 161-167, Aug. 15, 1981.

ORIGINAL PAGE IS
OF POOR QUALITY

**Table 1. $K_A$-and X-band atmospheric models for Goldstone (30-deg elevation angle)**

| | | | | | | | | | |
|---|---|---|---|---|---|---|---|---|---|
| 1. | Cumulative distribution (% time) | 0 | 50 | 80 | 90 | 95 | 98 | 99 | 99.5 |
| 2. | $K_A$-band noise temperature model, K | 9.84 | 19 | 25 | 29 | 35 | 43 | 53 | 69 |
| 3. | $K_A$-band water vapor, cloud, rain contribution, K | 0 | 9.16 | 15.16 | 19.16 | 25.16 | 33.16 | 43.16 | 59.16 |
| 4. | Water vapor, clouds, rain, modelled to X-band, K | 0 | 0.65 | 1.07 | 1.35 | 1.77 | 2.34 | 3.04 | 4.17 |
| 5. | X-band total noise temperature, K | 3.54 | 4.19 | 4.61 | 4.89 | 5.31 | 5.88 | 6.58 | 7.71 |
| 6. | $K_A$-band attenuation, dB | 0.15 | 0.29 | 0.39 | 0.45 | 0.54 | 0.67 | 0.82 | 1.07 |
| 7. | X-band attenuation, dB | 0.05 | 0.06 | 0.07 | 0.076 | 0.082 | 0.09 | 0.10 | 0.12 |
| 8. | $K_A$-band system noise temperature, K | 25.84 | 35 | 41 | 45 | 51 | 59 | 69 | 85 |
| 9. | X-band system noise temperature, K | 21.54 | 22.19 | 22.61 | 22.89 | 23.31 | 23.88 | 24.58 | 25.71 |
| 10. | $K_A$-band attenuation above baseline, dB | 0 | 0.14 | 0.24 | 0.30 | 0.39 | 0.51 | 0.67 | 0.92 |
| 11. | X-band attenuation above baseline, dB | 0 | 0.01 | 0.02 | 0.026 | 0.032 | 0.04 | 0.05 | 0.07 |
| 12. | ΔSNR, $K_A$-band, dB | 0 | 1.46 | 2.24 | 2.71 | 3.34 | 4.10 | 4.94 | 6.09 |
| 13. | ΔSNR, X-band, dB | 0 | 0.14 | 0.23 | 0.29 | 0.37 | 0.49 | 0.62 | 0.84 |
| 14. | $K_A$-band link SNR relative to X-band, dB | −0.89 | −2.21 | −2.90 | −3.31 | −3.86 | −4.51 | −5.20 | −6.14 |
| 15. | Net $K_A$-band link SNR advantage relative to X-band (11.51 dB + line 14) | 10.62 | 9.30 | 8.61 | 8.20 | 7.65 | 7.00 | 6.31 | 5.37 |

**Table 2. 1985-era DSN receiving system noise temperatures (30-deg elevation angle)**

| Contributor | $K_A$-band | X-band |
|---|---|---|
| Maser and plumbing, K | 7.3 | 8.9 |
| Cosmic background, K | 2.2 | 2.6 |
| Ground radiation, K | 6.5 | 6.5 |
| Total | 16.0 | 18.0 |

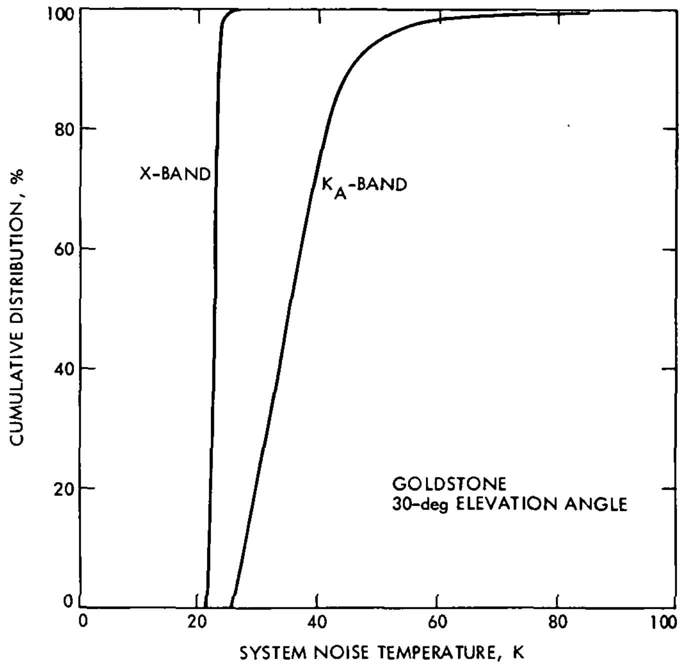


**Fig. 1. Cumulative distribution of X- and $K_A$-band system noise temperature for Goldstone, 30-deg elevation angle (see Table 1, Lines 8 and 9)**

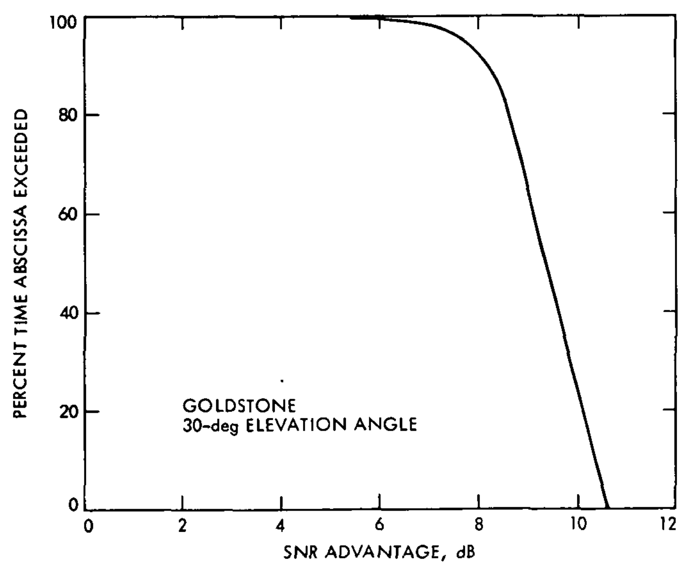


**Fig. 2. Distribution of $K_A$-band SNR advantage relative to X-band for Goldstone, 30-deg elevation angle (see Table 1, Line 15, and text)**